



Pressure tuning of the thermal conductivity of the layered muscovite crystal

Wen-Pin Hsieh,^{1,2,*} Bin Chen,³ Jie Li,³ Pawel Keblinski,⁴ and David G. Cahill^{2,5}

¹*Department of Physics, University of Illinois, Urbana, Illinois 61801, USA*

²*Frederick-Seitz Materials Research Laboratory, University of Illinois, Urbana, Illinois 61801, USA*

³*Department of Geology, University of Illinois, Urbana, Illinois 61801, USA*

⁴*Department of Materials Science and Engineering, Rensselaer Polytechnic Institute, Troy, New York 12180, USA*

⁵*Department of Materials Science and Engineering, University of Illinois, Urbana, Illinois 61801, USA*

(Received 13 October 2009; published 20 November 2009)

The physics of heat conduction in layered, anisotropic crystals is probed by measurements of the cross-plane elastic constant C_{33} and thermal conductivity Λ of muscovite mica as a function of hydrostatic pressure. Picosecond interferometry and time-domain thermoreflectance provide high-precision measurements of C_{33} and Λ , respectively, of micron-sized samples within a diamond-anvil cell; Λ changes from the anomalously low value of $0.46 \text{ W m}^{-1} \text{ K}^{-1}$ at ambient pressure to a value more typical of oxides crystals with large unit cells, $6.6 \text{ W m}^{-1} \text{ K}^{-1}$, at $P=24 \text{ GPa}$. Most of the pressure dependence of Λ can be accounted for by the pressure dependence of the cross-plane sound velocities.

DOI: [10.1103/PhysRevB.80.180302](https://doi.org/10.1103/PhysRevB.80.180302)

PACS number(s): 65.40.-b

I. INTRODUCTION

Recently, ultralow thermal conductivity—i.e., thermal conductivity Λ significantly lower than predicted by the model of the minimum thermal conductivity—was observed in disordered layered crystals.¹ A subsequent theoretical study suggested that a high degree of elastic anisotropy plays a critical role in suppressing the thermal conductivity in the cross-plane direction.² Measurements of the thermal conductivity as a function of pressure enable a critical test of this idea by enabling a continuous tuning of the anisotropy of the elastic constants; typically, the softer elastic constant in the cross-plane direction of a layered crystal has a higher anharmonicity and therefore increases more rapidly with pressure than the stiffer in-plane elastic constants.

Low thermal conductivity in layered crystals may find applications in improving thermal barriers and materials for thermoelectric energy conversion.^{3–6} We have chosen a prototypical layered crystal, muscovite mica, for these initial studies. Even though the layered structure of muscovite is not disordered, Λ in the cross-plane direction is extremely small for an oxide, $0.46 \text{ W m}^{-1} \text{ K}^{-1}$,^{7,8} a factor of ≈ 2 smaller than the predicted minimum thermal conductivity in the cross-plane direction, $0.9 \text{ W m}^{-1} \text{ K}^{-1}$. (The longitudinal and transverse speeds of sound in the cross-plane direction at ambient pressure, $v_l=4.5 \text{ km s}^{-1}$ and $v_t=2.4 \text{ km s}^{-1}$, were calculated from the elastic constants $C_{33}=58.6 \text{ GPa}$, $C_{44}=16.5 \text{ GPa}$,⁹ and mass density $\rho=2.83 \text{ g cm}^{-3}$. The atomic density is $n=8.26 \times 10^{22} \text{ cm}^{-3}$.) The thermal conductivity at ambient pressure is also highly anisotropic; the in-plane thermal conductivity is $\approx 4 \text{ W m}^{-1} \text{ K}^{-1}$.⁷

To obtain high-precision data for Λ at high pressures, an advance in experimental methods was required. The pressure dependence of the thermal conductivity of solids has been extensively studied at pressures up to $\approx 2 \text{ GPa}$.^{10–14} However, much higher pressures, $\approx 20 \text{ GPa}$, are needed to significantly alter the anisotropy of a layered oxide crystal. Studies of Λ up to or beyond 20 GPa are rare in the scientific literature and are essentially limited to studies of molecular

crystals;¹⁵ and relatively recent work applying the Ångström method within a 5000-ton multianvil apparatus¹⁶ and flash diffusivity within a diamond-anvil cell.¹⁷ Here, we present our study of the cross-plane elastic constant C_{33} and thermal conductivity of an anisotropic layered crystal, muscovite mica, from ambient pressure to 24 GPa using optical pump-probe methods combined with the diamond-anvil cell techniques.¹⁸

II. EXPERIMENTAL DETAILS

A sheet of $\sim 20\text{-}\mu\text{m}$ -thick muscovite mica, $\text{KAl}_2(\text{Si}_3\text{Al})\text{O}_{10}(\text{OH})_2$ (grade V-1 from SPI Supplies), was first coated with an Al film of $\sim 80 \text{ nm}$ thick and loaded, together with a small crystal of ruby, into a diamond-anvil cell (DAC) with culet size of $\approx 500 \mu\text{m}$ and pressurized by high-pressure gas loading with Ar (Ref. 19) (see Fig. 1). (The schematic unit cell of muscovite is shown in Ref. 9.) Hydrostatic pressure was determined by ruby fluorescence.¹⁸ The cross-plane thermal conductivity Λ of muscovite was measured at room temperature by time-domain thermoreflectance

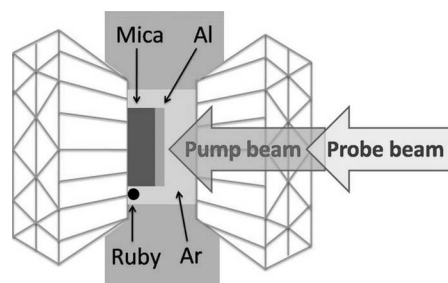


FIG. 1. Schematic drawing of the pump-probe optical measurements (TDTR and picosecond interferometry) of a muscovite sample in a diamond-anvil cell. An Al thin film serves as a transducer that absorbs energy from the pump beam and enables measurements of temperature through changes in optical reflectivity. The pressure medium is Ar.

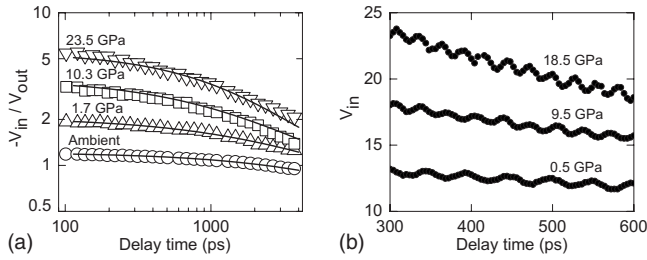


FIG. 2. (a) Example data for the ratio V_{in}/V_{out} as a function of delay time and fits (solid lines) to the heat-flow model of Ref. 25; data and fits are labeled by the pressure. (b) Example data for the oscillations in V_{in} as a function of delay time that are used to measure the Brillouin frequency of muscovite.

(TDTR).^{20–22} In the TDTR measurement, the output of a mode-locked Ti:sapphire laser was split into a pump beam, which heats the surface of the Al film on the muscovite sample, and a probe beam, which subsequently examines the resulting changes in reflectivity due to changes in temperature of the Al film.²³ The in-phase V_{in} and out-of-phase V_{out} components of the small variation of the reflected probe beam intensity that are synchronous with the 10 MHz modulation frequency of the pump beam were measured by a photodiode detector and rf lock-in amplifier. We found the thermorefectance of Al at 785 nm crosses through zero at $P \approx 6$ GPa (Ref. 24); we used a laser wavelength of 765 nm to obtain data near this pressure. (At 765 nm, the thermorefectance of Al is zero near $P \approx 8$ GPa.)

To determine the cross-plane thermal conductivity of muscovite, we compared the ratio V_{in}/V_{out} as a function of delay time to calculations using a thermal model²⁵ that was modified to take into account heat flow into the muscovite as well as into the Ar pressure medium.²⁶ The thermal penetration depth at the modulation frequency of the pump beam is 50–200 nm, small compared to the radius of the laser spot size, 7.5 μm , and heat flow is predominately one dimensional in the cross-plane direction. Example data and fits to the thermal model are shown in Fig. 2(a).

The thermal model has many parameters—laser spot size, Al film thickness, thermal conductivity, and heat capacity of each layer—but the thermal conductivity of muscovite is the only significant unknown. The thickness of Al was determined by picosecond acoustics. The pressure dependent thermal conductivity of Ar at room temperature was taken from recently published computer simulations.²⁷ Because the thermal conductivities of muscovite and Ar are small, the thermal model is insensitive to the thermal conductance G of the Al interfaces. We set $G=200 \text{ MW m}^{-2} \text{ K}^{-1}$ for the Al/muscovite interface and find that the data can be fit well using $G=80 \text{ MW m}^{-2} \text{ K}^{-1}$ for the Al/Ar interface at low pressures while at high pressures $G=200 \text{ MW m}^{-2} \text{ K}^{-1}$ provides the best fit. Therefore, we linearly scale the pressure dependence of thermal conductance of Al/Ar interface by $G=70+5.2P \text{ MW m}^{-2} \text{ K}^{-1}$, where P is the pressure in GPa.

The heat capacities of Al, muscovite, and Ar at high pressures are not known; therefore, we estimate the pressure dependence of the heat capacities from data for the pressure dependence of the atomic density and elastic constants. Because of the relatively low Debye temperature of Ar, we fix

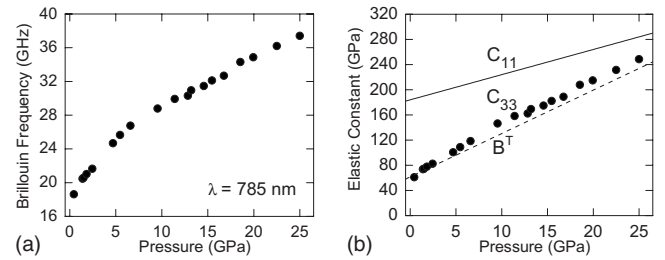


FIG. 3. Pressure dependence of the (a) Brillouin frequency and (b) C_{33} of the muscovite. C_{33} is derived from the Brillouin frequency data using the equation of state of muscovite and assuming that the index of refraction follows the Lorentz-Lorenz equation. The estimated $C_{11}=184 \text{ GPa}+4P$ and previously measured bulk modulus $B^T=61.4 \text{ GPa}+6.9P$ (Ref. 33) are plotted as solid and dashed line, respectively, for comparison.

the heat capacity per atom at the classical value: $C=1.36$, 1.86, and 2.16 $\text{J cm}^{-3} \text{ K}^{-1}$ at $P=2$, 10, and 20 GPa, respectively.²⁸ For Al, we assume that changes in the specific heat at high pressure can be estimated from the ambient pressure specific heat at reduced temperature; for example, at 10 and 20 GPa, the Debye temperature of Al increases by 24% and 43%,²⁹ respectively, and therefore we use the measured specific heats of Al at $T=242 \text{ K}$ and $T=210 \text{ K}$ to calculate the heat capacities at 10 and 20 GPa. For Al, the pressure dependence of atomic density n is stronger than the pressure dependence of the specific heat and the heat capacity per unit volume ($C=2.42 \text{ J cm}^{-3} \text{ K}^{-1}$ at ambient pressure) increases by 5% at 10 GPa and 9% at 20 GPa.^{30,31} For muscovite, we use data for the pressure dependence of elastic constants of MgSiO_3 (Ref. 32) to estimate the changes in the Debye temperature. (MgSiO_3 has nearly the same average atomic weight as muscovite and the temperature dependence of the specific heats are nearly identical over a wide temperature range.³⁰) By this calculation, the heat capacity of muscovite ($C=2.3 \text{ J cm}^{-3} \text{ K}^{-1}$ at ambient pressure) increases by 9% at 10 GPa and 15% at 20 GPa. The density of muscovite increases by 11.5% at 10 GPa and 20% at 20 GPa.³³

The elastic constants of minerals are often measured by inelastic light-scattering: inelastic light scattering from acoustic modes is typically referred to as Brillouin scattering and the frequency shift of the scattered light is known as the Brillouin frequency f . For longitudinal modes in a back-scattering geometry, $f=2Nv/\lambda$, where N is the index of refraction, v the longitudinal speed of sound, and λ the laser wavelength. In our experiments, we measured f of muscovite by picosecond interferometry.^{34,35} Thermal expansion of Al created by heating by the pump-laser pulses generates a strain pulse; interference of probe pulses reflected from the strain pulse and the Al surface creates periodic oscillations of frequency f in the in-phase signal V_{in} [see Fig. 2(b)].

III. RESULTS AND DISCUSSION

Figure 3(a) shows the pressure dependence of f . To determine the corresponding cross-plane elastic constant C_{33} shown in Fig. 3(b), we calculated the pressure dependence of the density ρ from the equation of state of muscovite³³ and

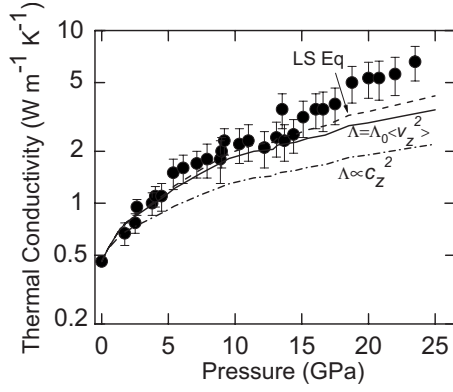


FIG. 4. Measurements (solid symbol) and theoretical predictions of the cross-plane thermal conductivity Λ of muscovite as a function of pressure. Error bars on the data points are dominated by uncertainties in the parameters in the thermal model used to analyze the data. The predicted Λ based on a constant relaxation time and an anisotropic Debye model [Eq. (1)] is shown as a solid line; and the dashed-dot line shows the scaling $\Lambda \propto c_z^2$. The difference between the scaling predicted by Eq. (1) and the scaling $\Lambda \propto c_z^2$ is the contribution to the pressure dependence of Λ due to changes in elastic anisotropy. The prediction of the LS equation using the scaling $\omega_D \propto \sqrt{C_{33}}$ is shown as a dashed line.

calculated the index N using the Lorentz-Lorenz formula $(N^2 - 1)/[\rho(N^2 + 2)] = A$, where A is a constant.³⁶ At ambient pressure, $N = 1.56$, $\rho = 2.83 \text{ g cm}^{-3}$, and $A = 0.114$; N increases by 4.8% at 10 GPa and 9% at 20 GPa.

We cannot measure the pressure dependence of the in-plane elastic constant C_{11} in our apparatus but if we assume that $dC_{11}/dP \approx 4$, a typical value for many silicates,^{37,38} $C_{11} = 184 \text{ GPa} + 4P$ and $C_{33} \approx C_{11}$ at the upper end of our pressure range [see Fig. 3(b)]. As muscovite is compressed, the decreasing interplanar distance increases the force constants of the interaction between the silicate layers.³⁶

Figure 4 shows the pressure dependence of the cross-plane thermal conductivity Λ of muscovite; Λ increases monotonically with pressure¹⁴ and increases by a factor of ≈ 3 and ≈ 15 at a pressure of 5 and 24 GPa, respectively. This data set includes measurements for both increasing and decreasing pressure. We also measured the thermal conductivity at ambient pressure after unloading the cell and obtained the same value, $0.46 \text{ W m}^{-1} \text{ K}^{-1}$, as we obtained before the muscovite was compressed. Thus, the changes in thermal conductivity are fully reversible and we have not observed significant hysteresis in the data. Our measurements do not support a previous report of a crystal-to-amorphous transition in muscovite at $P \geq 20 \text{ GPa}$.³³

We compare the thermal-conductivity data to two simple models. First, we consider the thermal conductivity in the relaxation-time approximation, $\Lambda = C\langle v_z^2 \rangle \tau$, where C is the heat capacity per unit volume of the vibrational modes that contribute significantly to heat transport, τ is the relaxation time, and $\langle v_z^2 \rangle$ is the average of the square of the cross-plane components of the group velocities of the vibrational modes. If we can assume the heat capacity and relaxation time are weakly dependent on pressure, changes in Λ are only the result of changes in $\langle v_z^2 \rangle$.

In an anisotropic Debye model, the phonon dispersion is $\omega^2 = (k_x c_x)^2 + (k_y c_y)^2 + (k_z c_z)^2$, where k_i and c_i are the wave vector and speed of sound along the i direction. The group velocity in the cross-plane direction is $v_z = \partial\omega / \partial k_z$. With $c_x = c_y$,

$$\langle v_z^2 \rangle = c_z^2 \int_0^{\pi/2} \frac{c_z^2 \cos^2 \theta}{c_x^2 \sin^2 \theta + c_z^2 \cos^2 \theta} \sin \theta d\theta. \quad (1)$$

To evaluate Eq. (1), since $c_x^2 = C_{11}/\rho$ and $c_z^2 = C_{33}/\rho$, we assume the pressure dependence of c_x^2 and c_z^2 follows the pressure dependence of C_{11} and C_{33} . The solid line in Fig. 4 shows the predicted Λ using $\langle v_z^2 \rangle$ from Eq. (1) and a fit to Λ at ambient pressure; i.e., $\Lambda = \Lambda_0 \langle v_z^2 \rangle$, with $\Lambda_0 = 4.2 \times 10^{-8} \text{ J s m}^{-3} \text{ K}^{-1}$. We cannot exclude the effects of changes in relaxation time with pressure, but the good agreement between the data and the prediction based on Eq. (1) suggests that most of the pressure dependence of Λ can be accounted for by changes in the sound velocities.

The good agreement between the data and this simple model also suggests that acoustic phonons are the dominant heat carriers in the cross-plane direction in muscovite. In most nonmetallic crystals, acoustic phonons are known to be the dominant heat carriers but this conclusion is not obviously true for the cross-plane direction of muscovite because the thermal conductivity is much smaller than the predicted minimum value and only a minority of the vibrational modes are acoustic modes with large group velocities.

The Leibfried-Schlömann (LS) equation—often used to model the pressure dependence of Λ —can also describe the data,

$$\Lambda = A \frac{V^{1/3} \omega_D^3}{\gamma T}, \quad (2)$$

where V is the volume, ω_D the Debye frequency, γ the Grüneisen constant, T the temperature, and A is a constant that is independent of pressure.³⁹ If we model the pressure dependence of ω_D through the pressure dependence of C_{33} , i.e., $\omega_D \propto \sqrt{C_{33}}$, then the prediction of Eq. (2) scales approximately as $C_{33}^{3/2}$ and is also in good agreement with the data (see Fig. 4). [The Grüneisen constant for longitudinal modes in the cross-plane direction, $\gamma = (1/2)dC_{33}/dP \approx 3.8$, is approximately independent of pressure.] We note, however, that the scaling $\omega_D \propto \sqrt{C_{33}}$ is difficult to justify since the LS equation is derived for an isotropic crystal.

IV. CONCLUSION

In conclusion, we have combined the techniques of picosecond interferometry, time-domain thermoreflectance, and the diamond-anvil cell to investigate the pressure dependence of thermal conductivity at pressures sufficiently high to significantly alter the anisotropy of a prototypical layered crystal, muscovite. The approach we have developed is general and applicable to any material that can be prepared with a smooth surface, coated with a metal film, and loaded into a diamond-anvil cell. While these initial studies are limited to room temperature, we anticipate that the upper temperature range of the measurements will only be limited by the physical and chemical stability of the metal film.

ACKNOWLEDGMENTS

This work was supported by the U.S. Air Force Office of Scientific Research (Grant No. MURI FA9550-08-1-0407), DOE and Carnegie Institution of Washington (Grant No. CDAC DOE CI JL 2008-05246), and National Aeronautics and Space Administration (Grant No. 655 NASA

NNX09AB946). W.-P. H. acknowledges support from National Science Council (Grant No. NSC-095-SAF-I-564-005-TMS) Taiwan, Republic of China. We thank Barbara Lavina for the help with the gas loading at GeoSoilEnviroCARS (Sector 13), Advanced Photon Source (APS), Argonne National Laboratory. The gas loading system is partially supported by COMPRES.

*whsieh2@illinois.edu

- ¹Catalin Chiritescu, David G. Cahill, Ngoc Nguyen, David Johnson, Arun Bodapati, Pawel Keblinski, and Paul Zschack, *Science* **315**, 351 (2007).
- ²L. Hu, P. Keblinski, S. Shenogin, and D. G. Cahill (unpublished).
- ³T. Kanno, S. Yotsuhashi, and H. Adachi, *Appl. Phys. Lett.* **85**, 739 (2004).
- ⁴Y. Shen, D. R. Clarke, and P. A. Fuierer, *Appl. Phys. Lett.* **93**, 102907 (2008).
- ⁵K. Takahata, Y. Iguchi, D. Tanaka, T. Itoh, and I. Terasaki, *Phys. Rev. B* **61**, 12551 (2000).
- ⁶I. Terasaki, H. Tanaka, A. Satake, S. Okada, and T. Fujii, *Phys. Rev. B* **70**, 214106 (2004).
- ⁷A. S. Gray and C. Uher, *J. Mater. Sci.* **12**, 959 (1977).
- ⁸R. W. Powell and E. Griffiths, *Proc. R. Soc. London, Ser. A* **163**, 189 (1937).
- ⁹M. T. Vaughan and S. Guggenheim, *J. Geophys. Res.*, [Solid Earth Planets] **91**, 4657 (1986).
- ¹⁰D. Gerlich, *J. Phys. C* **15**, 4305 (1982).
- ¹¹A. M. Hofmeister, *Proc. Natl. Acad. Sci. U.S.A.* **104**, 9192 (2007).
- ¹²S. W. Kieffer, *J. Geophys. Res.* **81**, 3025 (1976).
- ¹³S. W. Kieffer, I. C. Getting, and G. C. Kennedy, *J. Geophys. Res.* **81**, 3018 (1976).
- ¹⁴R. G. Ross, P. Andersson, B. Sundqvist, and G. Backstrom, *Rep. Prog. Phys.* **47**, 1347 (1984).
- ¹⁵E. H. Abramson, J. M. Brown, and L. J. Slutsky, *J. Chem. Phys.* **115**, 10461 (2001).
- ¹⁶Yousheng Xu, Thomas J. Shankland, Sven Linhardt, David C. Rubie, Falko Langenhorst, and Kurt Klasinski, *Phys. Earth Planet. Inter.* **143-144**, 321 (2004).
- ¹⁷Pierre Beck, Alexander F. Goncharov, Viktor V. Struzhkin, Burkhard Militzer, Ho-kwang Mao, and Russell J. Hemley, *Appl. Phys. Lett.* **91**, 181914 (2007).
- ¹⁸H. K. Mao, P. M. Bell, J. W. Shaner, and D. J. Steinberg, *J. Appl. Phys.* **49**, 3276 (1978).
- ¹⁹Mark Rivers, Vitali B. Prakapenka, Atsushi Kubo, Clayton Pulins, Christopher M. Holl, and Steven D. Jacobsen, High Press. Res. **28**, 273 (2008).
- ²⁰C. A. Paddock and G. L. Eesley, *J. Appl. Phys.* **60**, 285 (1986).
- ²¹D. A. Young, C. Thomsen, H. T. Grahn, H. J. Maris, and J. Tauc, in *Phonon Scattering in Condensed Matter*, edited by A. C. Anderson and J. P. Wolfe (Springer, Berlin, 1986).
- ²²David G. Cahill, Wayne K. Ford, Kenneth E. Goodson, Gerald D. Mahan, Arun Majumdar, Humphrey J. Maris, Roberto Merlin, and Simon R. Phillpot, *J. Appl. Phys.* **93**, 793 (2003).
- ²³Kwangu Kang, Yee Kan Koh, Catalin Chiritescu, Xuan Zheng, and David G. Cahill, *Rev. Sci. Instrum.* **79**, 114901 (2008).
- ²⁴R. G. Dandrea and N. W. Ashcroft, *Phys. Rev. B* **32**, 6936 (1985).
- ²⁵D. G. Cahill, *Rev. Sci. Instrum.* **75**, 5119 (2004).
- ²⁶Z. B. Ge, D. G. Cahill, and P. V. Braun, *Phys. Rev. Lett.* **96**, 186101 (2006).
- ²⁷K. V. Tretyakov and S. Scandolo, *J. Chem. Phys.* **121**, 11177 (2004).
- ²⁸Hiroyasu Shimizu, Hideyuki Tashiro, Tetsuji Kume, and Shigeo Sasaki, *Phys. Rev. Lett.* **86**, 4568 (2001).
- ²⁹W. P. Binnie, *Phys. Rev.* **103**, 579 (1956).
- ³⁰*Thermophysical Properties of High Temperature Solid Materials*, edited by Y. S. Touloukian (Purdue University, West Lafayette, IN, 1967), p. 4.
- ³¹C. Bercegeay and S. Bernard, *Phys. Rev. B* **72**, 214101 (2005).
- ³²R. M. Wentzcovitch, B. B. Karkia, S. Karatob, and C. R. S. Da Silva, *Earth Planet. Sci. Lett.* **164**, 371 (1998).
- ³³J. Faust and E. Knittle, *J. Geophys. Res.*, [Solid Earth] **99**, 19785 (1994).
- ³⁴K. E. O'Hara, X. Y. Hu, and D. G. Cahill, *J. Appl. Phys.* **90**, 4852 (2001).
- ³⁵C. Thomsen, H. T. Grahn, H. J. Maris, and J. Tauc, *Opt. Commun.* **60**, 55 (1986).
- ³⁶L. E. McNeil and M. Grimsditch, *J. Phys.: Condens. Matter* **5**, 1681 (1993).
- ³⁷M. Matsui and W. Busing, *Am. Mineral.* **69**, 1090 (1984).
- ³⁸R. Newnham and H. Yoon, *Mineral. Mag.* **39**, 78 (1973).
- ³⁹G. A. Slack, *Solid State Physics* (Academic, New York, 1979) Vol. 34, p. 35.